# Water-Entry Induced Cavity Pressure

**Minhyung Lee***
*School of Mechanical and Aerospace Engineering, Sejong University*

The pressure in a water-entry induced cavity, is analyzed up to the closed cavity (bubble). Water-entry is a highly transient phenomenon, and the evolution of the water-entry cavity must be explained by considering the entry speed, shape of the solid body, atmosphere pressure, and cavity pressure as the primary variables. This work is an extension of the cavity dynamics model recently reported by Lee (1997a). To extend the model for a wide range of entry speeds the cavity pressure is calculated from a one-dimensional quasi-steady flow model. The estimation of the cavity pressure allows us to explain the experimentally observed surface closure phenomena at low entry speeds. Predictions for the time of surface closure are compared with the published experimental data.

**Key Words** : Water-Entry, Surface Closure, Cavity Pressure

**Nomenclature**

| | |
|---|---|
| $A_o$ | : Projected area of a solid |
| $A(z)$, $B(z)$ | : Constants |
| $a$ | : Cavity radius |
| $C_d$ | : Velocity-dependent drag coefficient |
| $D$ | : Diameter |
| $E_p$ | : Kinetic energy |
| $g$ | : Gravitational acceleration |
| $m$ | : Air mass |
| $m_s$ | : Solid mass |
| $P_c$ | : Cavity pressure |
| $t$ | : Time |
| $t_b(z)$ | : Solid traveling time after entry |
| $u$ | : Internal energy |
| $U$ | : Moving velocity of a solid |
| $v$ | : Fluid radial velocity |
| $w$ | : Radial distance |
| $z$ | : Depth |
| $\beta$ | : Velocity decay constant |
| $\rho_w$ | : Fluid density |
| $\zeta$ | : Source strength |

* **E-mail** : mlee@sejong.ac.kr
**TEL** : +82-2-3408-3282 ; **FAX** : +82-2-3408-3333
School of Mechanical and Aerospace Engineering, Sejong University, 98 Kunja-dong, Kwangjin-gu, Seoul 143-747, Korea. (Manuscript **Received** October 7, 1999; **Revised** February 9, 2000)

## 1. Introduction

The problem of a solid body entering a semi-infinite free surface of water is a classical one and many interesting phenomena are discussed in the literature. Of particular interest are the physical events that occur at various stages of the entry that influence not only the solid motion but also the nature of induced ballistic waves in water (Lee, 1997b). Especially, the dynamics of the water-entry induced cavity is one of the important phenomena which has been studied extensively. This is due to the fact that the behavior of the solid body (missile) is strongly governed by the dynamics of the water-entry induced cavity. A detailed review of the dynamics of water-entry cavity for various speeds has been presented in a recent paper (Lee, 1997a). The cavity dynamics is discussed exclusively in the Philosophical Transactions of the Royal Society (1997). Gaudet (1998) proposed a simulated solution for the entry of circular disks, which has also been studied by several researchers.

The formation and collapse of the water-entry induced cavity depends on the physical properties of the solid body, gas and fluid that establish the forces that combine with gravity and inertia to determine transient entry phenomena (Waugh and Stubstad, 1972). The dominant mechanism governing the cavity formation is the kinetic energy transfer from the body to the cavity. The cavity wall continues to open until the pressure difference between the surrounding fluid and cavity forces the fluid to return to its undisturbed location. The gravitational effects can be neglected at high-speed.

According to Birkhoff and Zarantonello (1948) and Lee (1997a), there are five different cavity dynamics regimes: very low-speed regime, low-speed regime, transient regime, high-speed regime, and very high-speed regime. For a very low-speed entry ($20<\mathrm{Fr}<40$), the air flow filling the induced cavity is so fast that the pressure drop inside the cavity becomes small. Here, $\mathrm{Fr}=U_i^2/gD$, g is the gravitational acceleration, $U_i$ is the entry speed and $D$ is the characteristic length (e. g., the diameter of a sphere). That is, the cavity pressure can be assumed to be the atmosphere pressure. The same is true for entry from a vacuum. In these cases, the cavity closure occurs at a location far from the free-surface (deep closure). As the entry speed increases for roughly $\mathrm{Fr}>150$ (low-speed regime), the pressure drop in the cavity becomes so significant, at least near the cavity neck, that the closure occurs near the free-surface (surface closure). Deep closure is preceded by a surface closure. The surface closure is due to the under-pressure caused by the air flow into the cavity, referred to as the Bernoulli effect. However, as the speed increases further (transient regime through high-speed regime) the pressure in the cavity becomes the vapor pressure and no further decrease in cavity pressure is induced. Then the closure occurs again at deep location (Lee, 1997a). So, the cavity dynamics which influences the behavior of a solid in the fluid medium is strongly dependent on the cavity pressure.

In this paper, the dynamics of the water-entry cavity based on an energy balance model is first described. In order to apply the model to an entry from atmospheric pressure, a quasi-steady flow model for predicting the pressure inside the cavity is developed in Section 3. Then, the predicted time of surface closure is compared to experimental data in section 4. The final section summarizes this study and suggests directions for further research.

## 2. Cavity Dynamics Theory

We are interested in calculating the highly transient evolution of the flow due to a solid body impulsively accelerated at $t=0$ to an initial velocity $U_i$, moving into a semi-fluid medium. For consistency, the same symbols and notations to denote various quantities in the original article (Lee, 1997a) will also be used here. The geometry of the problem is sketched in Fig. 1. Since the solid body is decelerated by drag, the dynamics of a moving solid is governed by the kinetic energy loss (Lundstrom, 1971),

$$m_s\frac{d^2z}{dt^2}=m_s\frac{dU}{dt}=-\frac{1}{2}\rho_w A_o C_d U^2 \qquad (1)$$

where the properties are the mass of the solid $m_s$, moving axis $z$, time $t$, solid moving velocity $U$, fluid density $\rho_w$, projected area of the solid $A_o$, and velocity-dependent drag coefficient $C_d$. The rate of change of kinetic energy with respect to depth can then be expressed as,

$$\frac{dE_p}{dz}=-m_sU\frac{dU}{dz}=m_s\beta U^2 \qquad (2)$$

where $E_p=0.5\ m_sU^2$ and $\beta=\beta(U)=\frac{\rho_w A_o C_d}{2\ m_s}$ is a velocity decay constant (Charters, 1945).

Now, the influence of solid body motion on the cavity formation is estimated here. The fluid is assumed to be irrotational everywhere such that the solid body can be approximated as a moving

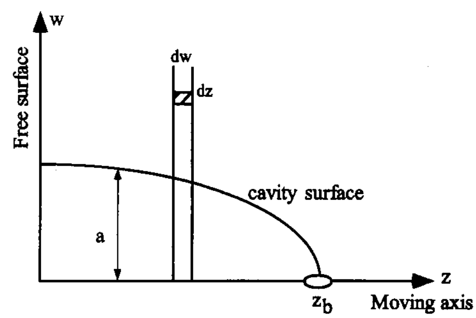


**Fig. 1** Cavity evolution model

source. The local fluid radial velocity is then related to source strength $\zeta(\xi, t)$ and radial distance $w$ as,

$$v = 2\zeta(\xi, t)/w \tag{3}$$

In order to determine the source strength, it is assumed that the kinetic energy loss of a solid body is transformed into the kinetic energy and potential energy of the fluid section (Birkhoff and Zarantonello, 1957). The energy balance equation based on the previous argument can be expressed as,

$$\left.\frac{dE_p}{dz}\right|_{\xi} dz = 4\pi\rho_w N\zeta^2 + \pi(P_o - P_c) \tag{4}$$

where, $P_c$ is the pressure in the cavity. The two terms on the right hand side of Eq. (4) represent kinetic and potential energies, respectively. By defining $P_g = (P_o - P_c)$ and introducing two terms,

$$[A(z)^2] = P_g\left[\frac{dE_p}{dz}\right]_{\xi}$$
$$[B(z)^2] = \frac{P_g}{\rho_w N} \tag{5}$$

the source strength is obtained as,

$$\zeta = \pm\frac{1}{2}B\sqrt{A(z)^2 - a^2} \tag{6}$$

where, $a$ is the cavity radius as a function of depth. Another boundary condition applied is the kinematic boundary condition at the cavity wall.

$$\zeta = \frac{1}{2}a\frac{da}{dt} \tag{7}$$

Finally, from Eqs. (6), (7) an equation of cavity dynamics is obtained,

$$a\frac{da}{dt} = \pm B\sqrt{A(z)^2 - a^2} \tag{8}$$

Integration of Eq. (8) allows us to determine the history of the cavity radius as a function of depth and time. As shown in the equations, the pressure inside the cavity is one of the important parameters governing the dynamics of the cavity.

## 3. Water-Entry Cavity Pressure

For entry in vacuum or at very low atmospheric pressure, the cavity pressure also remains at constant vacuum pressure. In this case, Eq. (8) can be integrated with the solid arrival time $t_b(z)$ (Eq. (1)) at each depth,

$$a(z) = \sqrt{A(z)^2 - [A(z) - B(t - t_b(z))]^2} \tag{9}$$

Equation (9) states that, at each depth, the cavity continues to expand until the pressure difference between the surrounding fluid and cavity interior balances the induced inertia effects. Then it starts to collapse and leads to a cavity closure. The cavity wall velocity along the depth can be determined by differentiating Eq. (9) with respect to time. Using this equation, the time of cavity collapse is estimated. Since each depth has a different collapse time, the time and location of deep closure is equal to the minimum value. Some results for this case are described in the previous work (Lee, 1997a), and the deep closure process is displayed in Fig. 2.

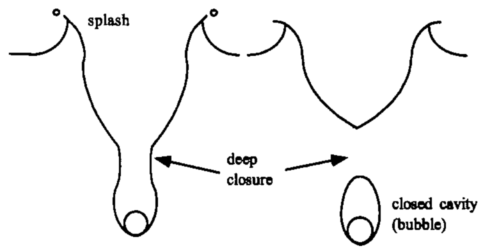


**Fig. 2** Deep closure at very reduced atmosphere pressure

For entry from an atmospheric pressure at low-speed, however, the analysis becomes considerably more complicated since it is necessary to calculate the pressure inside the cavity. The pressure may vary with depth and time. To the author's best knowledge, nothing regarding pressure gradients along depth direction is discussed in the literature. Therefore, the pressure is assumed to be a function of time. The pressure-time history is then estimated by the quasi-steady flow method proposed by Abelson (1969).

Consider a cavity as an expanding container into which air flows. The proposed one-dimensional cavity container model is shown in Fig. 3. This model will be applied to both open and closed cavity phases. The open cavity phase is described first. At each time, the cavity volume is

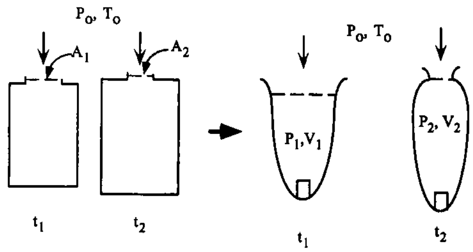


**Fig. 3** Cavity container analogy model

$V$, and the inside pressure is $P$. We apply the first law of thermodynamics for the system.

$$\Delta m h_o = W_{1-2} + (m_2 u_2 - m_1 u_1) \tag{10}$$

where $h_o$ is the stagnation enthalpy and $u$ is the internal energy. Assuming a quasi-steady expansion process ($W_{1-2} = p(V_2 - V_1)$) and the ideal gas relation ($PV = mRT$), we get a cavity pressure as a function of volume, air mass flow, and pressure at previous time.

$$P_2 = P_1 \frac{\dfrac{\Delta m\ a_o{}^2}{\gamma-1} + \left[\dfrac{V_2 - V_1}{2} + \dfrac{V_1}{\gamma-1}\right]}{\left[\dfrac{V_2 - V_1}{2} + \dfrac{V_2}{\gamma-1}\right]} \tag{11}$$

where $a_o$ is the speed of sound in air and $\gamma$ is equal to 1.4. $\Delta m (m_2 - m_1)$ is the air mass flow into the cavity during the time interval $\Delta t$, and can be expressed as,

$$\Delta m = \bar{\rho}_a \bar{u} \bar{A} \Delta t \tag{12}$$

where the barred quantities represent values average over the time interval, and $A$ refers to the cross-sectional area of the cavity aperture. One -dimensional flow approximation has been made here, although the entrance is not one-dimensional. If the steady-flow energy equation for an adiabatic process is applied to two points on a stream line, one point outside and far away from the container entrance and the other just at the entrance, the velocity is given by,

$$u = a_o \sqrt{\frac{2}{\gamma-1}\left[1 - \left(\frac{P}{P_o}\right)^{\frac{\gamma-1}{\gamma}}\right]} \tag{13}$$

where $P_o$ is the undisturbed pressure. By substituting the isentropic relation and Eq. (13) into Eq. (12), we obtain,

$$\Delta m = \rho_{a_o} a_o \left(\frac{P_1 + P_2}{2}\right)^{\frac{1}{\gamma}} \bar{A} \Delta t \sqrt{\frac{2}{\gamma-1}\left[1 - \left(\frac{P_1 + P_2}{2P_o}\right)^{\frac{\gamma-1}{\gamma}}\right]} \tag{14}$$

Now, it is necessary to obtain cavity volume as a function of time by integrating the cavity radius along z-direction. Using Eq. (10), the cavity volume is given by,

$$V = \pi \int_0^{z_b} a(z, t)^2 dz \tag{15}$$

Equations (11), (14), (15) should be simultaneously solved for $P_2$, $\Delta m$, and $V_2$ for the time interval $\Delta t$, with Eq. (9). The total time range of interest is divided into many intervals $\Delta t_n$, the equations are solved for each $\Delta t_i$ with $P_2$ and $V_2$ of the $i^{th}$ interval, which becomes $P_1$ and $V_1$ of the $i+1^{th}$ interval. In this way, a quasi-steady solution for the inside cavity pressure as a function of time is obtained for an unsteady process. Initially, the cavity pressure is taken to be $P_o$.

At a later stage, as previously mentioned, the cavity collapses and becomes a closed cavity (bubble). Even for this stage, the cavity can be described with a simplification of the current method. In this case there is no longer air flow into the cavity ($\Delta m = 0$), so Eq. (11) becomes,

$$P_2 = \frac{\left[\dfrac{V_2 - V_1}{2} + \dfrac{V_1}{\gamma-1}\right]}{\left[\dfrac{V_2 - V_1}{2} + \dfrac{V_2}{\gamma-1}\right]} P_1 \tag{16}$$

For the cavity pressure and volume, this equation need be solved with Eq. (15). Note that an adiabatic process has been assumed in the above analysis because heat transfer to the cavity should be negligible. In Eq. (16), the mass of air inside the cavity should remain constant. That mass is conserved until another cavity closure which separates the bubble into two parts. Hence, the current analysis is valid until another cavity closure is initiated. A further analysis is difficult, if possible at all, to estimate the amount of air remaining in each bubble.

Figure 4 shows the cavity pressure and volume for the entry of a 7.63 cm diameter, 140° conical-nosed projectile at velocity of 45 m/s. Initially, the cavity pressure decreases due to the air flow (Bernoulli effects) and then increases slightly after surface closure since there is no air flow after

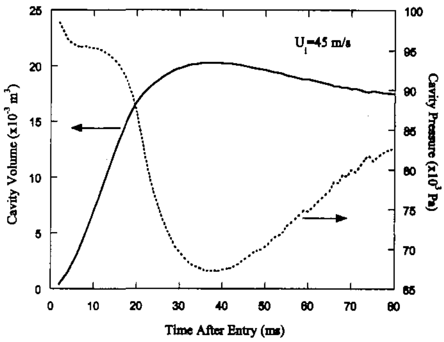


**Fig. 4** Cavity pressure-cavity volume for the entry of a 7.64 cm diameter, 140° conical-nosed projectile at velocity of 45 m/s

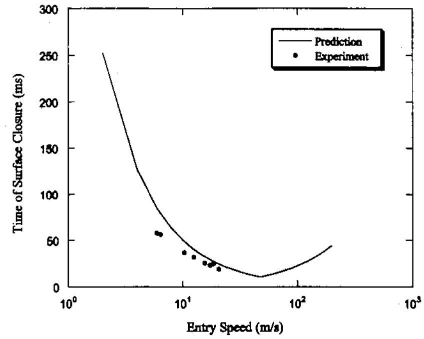


**Fig. 5** The time of surface closure versus entry speed. The atmosphere pressure is 0.25 atm. the solid circle data from Gilbarg et al., (1948)

the closure. Compared to the experimental data obtained by Abelson (1970), the minimum pressure occurs at a slightly later time. The cavity volume shows the other trend. Once the cavity closure occurs at the entrance and there is no further air flow, the volume increases due to the momentum imparted to the cavity wall. After the minimum pressure (at maximum volume), the pressure starts to increase and the volume decreases. Eventually, cavities which show pressure oscillations dissipate through a pinching process. Some correlations for these processes are obtained by Wolfe (1988).

## 4. Time of Surface Closure

The two major forces leading to surface closure are those due to the under-pressure caused by the flow of air into the cavity behind the entry body, referred to as the Bernoulli effect, and surface tension. The air rushing into the cavity causes a local under-pressure, frequently estimated by $1/2\ \rho_a U_i^2$, where $\rho_a$ is the air density. However, Abelson (1970) measured that the cavity pressure drop is an order of magnitude greater than this assumption. This under-pressure causes the neck to contract until a complete surface closure occurs.

The time of surface closure is obtained using the present model with the assumption that the pressure drop at least in the splash neck is equal to $1/2n\ \rho_a U_i^2$, where $n$ is a constant determined from experimental data. Figure 5 displays the time of surface closure for the entry of 1-inch sphere from reduced atmosphere pressure. The experimental data (Gilbarg and Abelson, 1948) are also displayed. Unfortunately, no comparison is made for a high-speed entry because no data are available. If the model presented here is adequate, then the time of surface closure for different entry cases can be represented by the same parameters. The correlated value of $n$ here is 300. For this value of $n$, the cavity pressure becomes vacuum at the entry speed of 51 m/s. Even though the entry speed is larger than this value, there is no further decrease in the cavity pressure. Thurs, the time of surface closure starts to increase for entry speeds larger than 51 m/s. This is due to the fact that as the entry speed increases, a momentum deposition from the moving body into the cavity increases while the pressure drop remains one atmosphere pressure. Actually, in this case, a deep closure occurs prior to the surface closure.

Figure 6 shows the time of surface closure ($T_s$) for sphere entries from reduced atmospheric pressures. The experimental data for low-speed entry (Gilbarg and Anderson, 1948) are also displayed. For different atmospheric pressures, the model predictions compare well with the experimental results.

A possible scaling for the time of surface closure is investigated using the current model, and and the results are compared with the previous analysis. The time of surface closure is given by

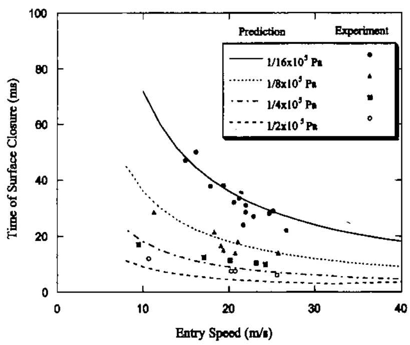


**Fig. 6** Time of surface closure versus entry speed, 1. 27 cm sphere at reduced atmosphere pressure

Lee (1997a),

$$T_s = 2\frac{A(z)}{B} = \frac{2U_i}{(P_o - P_c)}\sqrt{\frac{\rho_w N}{\pi} m_s \beta} \quad (17)$$

If the pressure drop at the cavity neck is constant and determined by the Bernoulli effects, we can then obtain the following result by substituting decay constant $\beta$. This is the same result given by Birkhoff and Issacs (1951).

$$\frac{\rho_a\ U_i\ T_s}{D} = constant \quad (18)$$

## 5. Conclusions

The dynamics of water-entry induced cavity and cavity pressure are studied analytically, and predictions are compared to the available experimental data. The understanding of the cavity dynamics is important because it plays a key role for the behavior of the water-entry body. The following conclusions can be drawn.

For the case of a low-speed entry, a surface closure is observed prior to a deep closure. As the entry speed increases further, the surface closure is preceded by the deep closure. We can explain this trend by two factors-the momentum transfer and Bernoulli effects. At low entry speeds the momentum transfer from the moving body into the cavity is small, however the pressure drop near the free surface is significant. As the entry speed increases, the pressure drop at the free surface stagnates while the momentum deposition does not. The analytical predictions for the time of surface closure compare well with the experimental data reported in the literature. Although the cavity pressure is predicted for the period from the entry to the closed cavity (bubble), more detailed analyes are required. The scaling for the time of surface closure was found from the present model and compared with previous analyses.

## Acknowledgment

This work was supported by Korea Research Foundation under contract number 1998-003-E00020.

## References

Abelson, H. I., 1969, The Behavior of the Cavity formed by a Projectile Entering the Water Vertically, The University of Maryland, Ph. D. Thesis.

Abelson, H. I., 1970, "Pressure Measurements in the Water-Entry Cavity," *J. Fluid. Mech.*, Vol. 44, No. 1, pp. 129～144.

Birkhoff, G. and Isaacs, R., 1951, "Transient Cavities in Air-Water Entry," NAVORD Report No. 1490.

Birkhoff, G. and Zarantonello, F. H., 1957, *Jets, Wakes, and Cavities*, Academic Press, New York.

Charters, A. C. and Thomas, R. N., 1945, "The Aerodynamic Performance of Small Spheres from Subsonic to High Speed Supersonic Velocities," *J. of Aeronaut. Sci.* Vol. 12, p. 468.

Gaudet, S., 1998, "Numerical Simulation of Circular Disks Entering the Free Surface of a Fluid," *Physics of Fluids*, Vol. 10, No. 10, pp. 2489～2499.

Gilbarg, D. & Anderson, R. A., 1948, "Influence of Atmospheric Pressure on the Phenomena Accompanying the Entry of Spheres into Water," *J. of Applied Physics*, Vol. 19, No. 2, pp. 127～139.

Lee, M., Longoria, R. G. and Wilson, D. E., 1997a, "Cavity Dynamics in High-Speed Water Entry," *Physics of Fluids*, Vol. 9, No. 3, pp. 540～550.

Lee, M., Longoria, R. G. and Wilson, D. E., 1997b, "Ballistic Waves in High-Speed Water

Entry," *J. of Fluids and Structures*, Vol. 11, pp. 819~844.

Lundstrom, E. A., 1971, "Fluid Dynamic Analysis of Hydraulic Ram," Naval Weapons Center, China Lake, CA, NWC TP 5227.

"Violent Surface Motion, " Philosophical Transactions: Mathematical, *Physical and Engineering Sciences, Series* A Vol. 355, (1724 15), 1997.

Waugh, G. & Stubstad, G. W., 1972, *Hydroballistics Modeling*, Naval Underwater Center, San Diego, CA., USA.

Wolfe, W. P. and Gutierrez, 1988, "Experimental Measurements of Pressure in Water-Entry Cavities," *Cavitation and Multiphase Flow Forum*, FED-Vol. 135, ASME, pp. 104~107.